PHYSICAL REVIEW C VOLUME 57, NUMBER 3 MARCH 1998

Dynamics of radial collective energy in near central collisions for 1*A* GeV Au+C

J. Lauret,[1] S. Albergo,[8] F. Bieser,[4] N. N. Ajitanand,[1] John M. Alexander,[1] F. P. Brady,[6] Z. Caccia,[8] D. Cebra,[6] A. D. Chacon,[7] J. L. Chance,[6] Y. Choi,[9] P. Chung,[1] S. Costa,[8] P. Danielewicz,[3] J. B. Elliott,[2] M. Gilkes,[1] J. A. Hauger,[2] A. S. Hirsch,[2] E. L. Hjort,[2] A. Insolia,[8] M. Justice,[5] D. Keane,[5] J. Kintner,[6] Roy A. Lacey,[1] V. Lindenstruth,[10] M. A. Lisa,[4] H. S. Matis,[4] R. McGrath,[1] M. McMahan,[4] C. McParland,[4] W. F. J. Müller,[10] D. L. Olson,[4] M. D. Partlan,[4] N. T. Porile,[2] R. Potenza,[8] G. Rai,[4] J. Rasmussen,[4] H. G. Ritter,[4] J. Romanski,[8] J. L. Romero,[6] G. V. Russo,[8] H. Sann,[10] R. Scharenberg,[2] A. Scott,[5] Y. Shao,[5] B. K. Srivastava,[2] T. J. M. Symons,[4] M. Tincknell,[2] C. Tuvè,[8] S. Wang,[5] P. Warren,[2] T. Wienold,[4] H. H. Wieman,[4] and K. Wolf[7]

(EOS Collaboration)

[1]*Departments of Chemistry and Physics, State University of New York at Stony Brook, Stony Brook, New York 11794-3400*

[2]*Department of Physics, Purdue University, West Lafayette, Indiana 47907*

[3]*NSCL and the Department of Physics, Michigan State University, East Lansing, Michigan 48824-1321*

[4]*Nuclear Science Division, Lawrence Berkeley National Laboratory, Berkeley, California 94720*

[5]*Department of Physics, Kent State University, Kent, Ohio 44242*

[6]*Department of Physics, University of California, Davis, California 95616*

[7]*Department of Physics, Texas A&M University, College Station, Texas 77843*

[8]*Università di Catania & INFN-Sezione di Catania, Catania, Italy 95129*

[9]*Sung Kyun University, Chun-Chun-Dong 300, Korea*

[10]*GSI, D-64220 Darmstadt, Germany*

(Received 27 June 1997)

Transverse kinetic energies of individual fragments have been measured over a broad range of emitter excitation energies for the reaction 1*A* GeV Au+C. For excitation energies leading to large intermediate mass fragment multiplicities, these transverse energies require large collective radial expansion of the emitting systems. However, the traditional decomposition of the transverse energy into a thermal component and a Coulomb and collective component proportional to the fragment mass cannot account for this expansion. Expansion velocities show an increase with decreasing fragment Z and thus indicate fractionation of the collective energy for the expanding system. This collective energy increases with emitter excitation up to about 50% of the energy deposited for a nuclear system with total energy $\sim 12A$ MeV. The bulk of the collective energy is carried away by ejectiles of $Z \leqslant 3$.
[S0556-2813(98)51103-X]

PACS number(s): 25.75.−q, 25.70.Pq

Violent collisions between heavy nuclei of 0.1−2*A* GeV are often termed multifragmentation due to the large number and variety of ejectiles. A good characterization of this process is widely believed to be a key step for the delimitation of the nuclear equation of state [1–3], as well as for understanding liquid-gas phase transitions in nuclei [4–8]. Central to a description of the mechanism for multifragmentation are the questions of ''achievement of equilibration'' and the associated role of collective nuclear expansion [9–15]. No one theoretical model is currently capable of addressing the complete reaction time sequence or the whole range of experimental observables. Therefore one must use several models and/or assumptions in conjunction to piece together a reasonable scenario. In this study of 1*A* GeV Au+C we explore the dynamical approach toward equilibration along with the associated collective expansion. We emphasize two observables: the fragment charge (or Z) distributions, and the transverse kinetic energies as a function of Z. Interpretations are based on dynamical calculations from the Boltzmann-Uehling-Uhlenbeck (BUU) model [16] and equilibrium model calculations from the Berlin multifragmentation model [17]. The picture that emerges [18] involves an extremely fast period ($\lesssim 25$ fm/c) of decidedly prethermal emission, then a fast period of collision-driven expansion ($\approx 25-50$ fm/c), with a termination by multifragmentation ($\sim 50-80$ fm/c) from a low density configuration near to or at equilibrium.

The data on which our analysis is based are reported in Refs. [19,20]. In that work, the authors present evidence for two reaction stages, a prompt stage in which light particles are ejected leading to the formation of an equilibrated remnant, which deexcites in a second stage. Here, we propose a dynamical scenario which is different from that of Ref. [19] for the early history, but not mutually exclusive for the equilibrium breakup phase. Our analysis reveals significant radial collective flow similar to that obtained from the energy conservation arguments made in Ref. [19].

The ^{197}Au beams ($E/A = 1$ GeV) used for these measurements were provided by the Lawerence Berkeley Laboratory Bevalac accelerator. Charged reaction products were detected with the EOS experimental setup. This setup includes a time projection chamber (TPC) [21], a multi sampling ionization chamber (MUSIC) [22], a time-of-flight wall, and a neutron spectrometer [23]. A carbon target was located near the entrance window of the active TPC volume to ensure essentially complete detection of all charged products in the EOS setup. Here, we report on events for which the average detected charge Z is approximately equal to the charge of the gold nucleus.

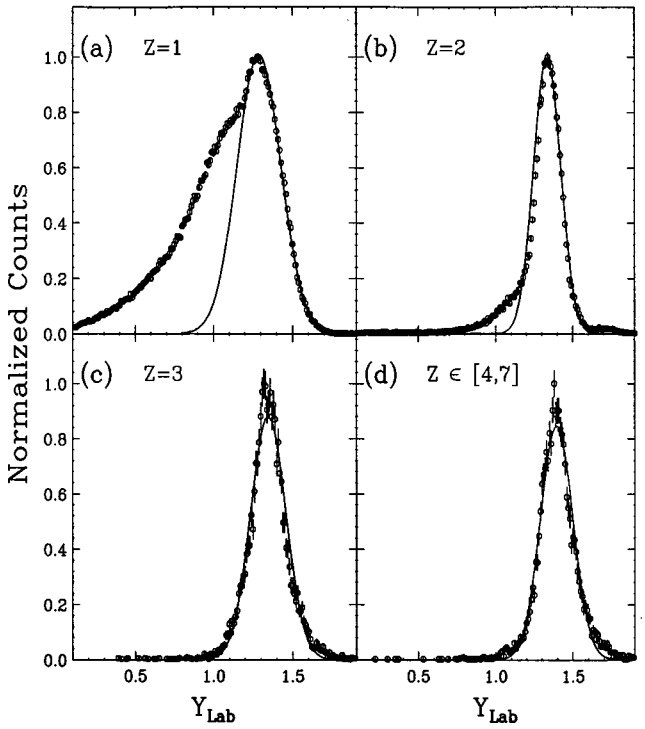

FIG. 1. Lab rapidity distributions for $Z=1$ (a), 2 (b), 3 (c), and 3–7 (d) [20]. The solid lines represent Gaussian curves drawn to guide the eye. Error bars here and below are from statistics only.

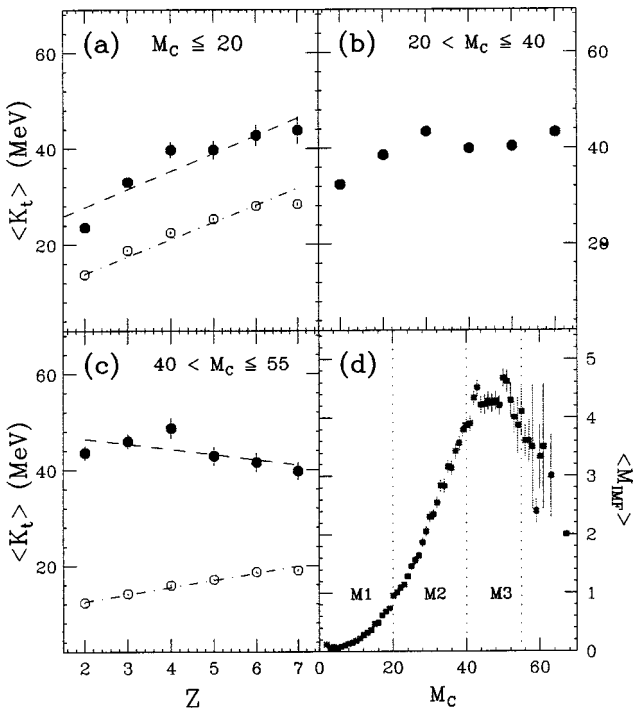

FIG. 2. Experimental (filled circles) and calculated (open circles) average transverse energy $\langle K_t\rangle$ vs Z. Results are shown for multiplicity bins $M1$ (a), $M2$ (b), and $M3$ (c). The dashed and dot-dashed lines represent fits to the experimental and calculated $\langle K_t\rangle$ values. Panel (d) shows the mean intermediate mass fragment multiplicity $\langle M_{\rm IMF}\rangle$ vs total charged particle multiplicity M_c. Dotted lines indicate the multiplicity bin selections. See Fig. 4 and the text for calculational inputs and sensitivities.

An important prerequisite for studying multifragmentation is to establish whether or not the emitted fragments are produced from a single emitting source ensemble. To this end, rapidity distributions for $Z=1$, 2, 3, and 4–7 fragments are shown in Fig. 1 [20]. The distributions shown for $Z=1$ and $Z=2$ fragments [Fig. 1(a) and Fig. 1(b)] exhibit asymmetries which are attributable to knockout ejection along the c.m. direction of the light C nucleus. In marked contrast, the rapidity distributions shown for the heavier fragments ($Z\geqslant 3$) in Figs. 1(c) and 1(d) show nearly Gaussian shapes which are commonly associated with a ''single'' emitting source ensemble. The average mass and energy of this source ensemble which has clearly lost memory of the beam direction will be discussed along with Fig. 3 below. For these systems, we use the mean transverse kinetic energies $\langle K_t\rangle = \sqrt{(p_t^2+m^2)}-m$ of the fragments to explore and characterize the role of collective expansion and the extent of thermalization (p_t and m represent the transverse momentum and mass of the fragments respectively).

Figure 2 shows the evolution of $\langle K_t\rangle$ with fragment Z and reaction violence. Panel (d) illustrates the, now familiar, rise and fall [24] of average intermediate mass fragments (IMF) multiplicity $\langle M_{\rm IMF}\rangle$ with charged-particle multiplicity M_c. Panels (a)–(c) [25] show the dependence of $\langle K_t\rangle$ on fragment Z for the three multiplicity gates indicated in Fig. 2(d). For the lowest multiplicity bin $M1$ [or lowest excitation energies], values of $\langle K_t\rangle$ show an increase with increasing ejectile charge. This is the trend expected for fragment energies which are mainly driven by Coulomb repulsion. When the multiplicity range is increased to bin $M2$, the trend of values for $\langle K_t\rangle$ changes to a relatively flat dependence on Z [Fig. 2(b)]. We interpret this change as evidence for two effects: (a) an increase in the thermal energy of the emitter which leads to an increase in $\langle M_{\rm IMF}\rangle$ and hence a decrease in the slope of the Z dependence of $\langle K_t\rangle$ and (b) significantly reduced Coulomb barriers due to radial expansion of the emitting source.

For the highest multiplicity gate ($M3$), which corresponds to multiplicities for which the mean number of IMF's is maximal, Fig. 2(c) even seems to show an inversion of the slope for the Z dependence of $\langle K_t\rangle$. These slope changes suggest the presence of a major driving force separate and different from the simplest Coulomb repulsions and thermal motions. The open points in Fig. 2 were calculated by the Berlin microcanonical statistical model for multifragmentation [17], which includes these Coulomb and thermal effects. This well documented model considers the statistical multiejectile breakup of a low density nuclear system with a given thermal excitation energy, $E_{\rm therm}$ (as discussed below). The large differences between experiment and calculation must be attributed to an additional driving force. We ascribe this driving force to radial collective expansion or flow.

To assign an average expansion velocity for each fragment charge, additional calculations were performed with the Berlin statistical model code [17]. This code uses the technique of Metropolis sampling to populate phase space and hence create sample configurations for fragment freeze-out for an emitting system of given mass, charge, and excitation energy. Energy, charge, and mass are conserved in every event, and the post-freeze-out kinematics are followed using N-body Coulomb trajectories. Secondary decay of the pri-

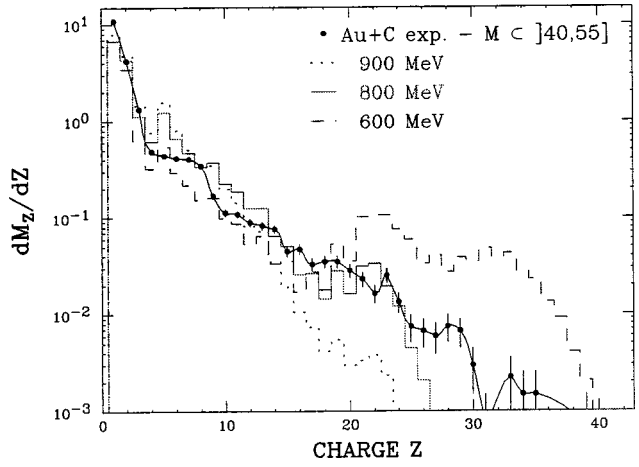

FIG. 3. Fragment Z distributions for 1A GeV Au+C. The solid histogram represents the experimental data for multiplicity bin $M3$. Dashed, dot-dashed, and dotted histograms represent calculated distributions for emitter $A=130$ with thermal excitation energies indicated in the figure. See text for results for $A=115$.

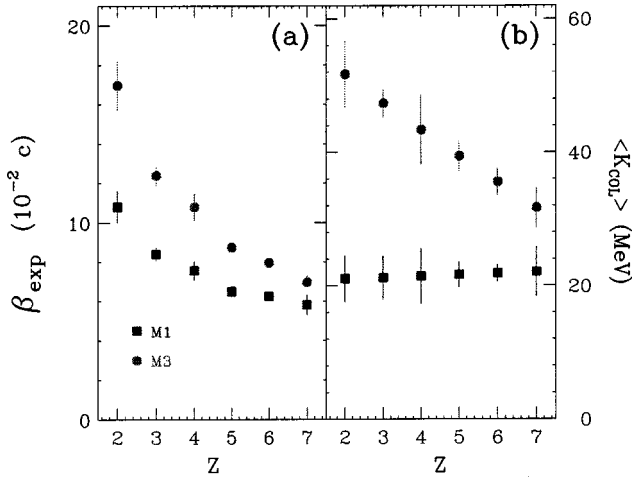

FIG. 4. Expansion velocity $\beta_{\rm exp}$ vs fragment Z. (a) Mean collective energy $\langle K_{\rm col}\rangle$ vs Z. (b) Results are shown for multiplicity bins $M1$ (filled squares) and $M3$ (filled circles). Inputs for multifragmentation calculations [17] were $M3$: $A=130$, $Z=54$, $E_{\rm therm}=800$, MeV (or $\langle T\rangle\simeq 5.2$ MeV); $M1$: $A=197$, $Z=79$, $E_{\rm therm}=500$ MeV (or $\langle T\rangle\simeq 3.5$ MeV). No important changes result from reasonable input changes (see text).

mary fragments are taken into account by considering the excited states of these fragments to be the product of several unbound single particle states times the bound states of the daughter residues [17]. To address the role of collective expansion, we modified the code to include a radial velocity boost for each of the fragments at freeze-out. The mass (A), charge (Z), and thermal excitation energy ($E_{\rm therm}$) of the emitting system are basic inputs for the microcanonical statistical model code. (Default radius values [$r_0=2.0$–2.2 fm] were used for the fragmentation volume, but no conclusions are significantly affected by this choice.) We have used experimental data to constrain the input values of A, Z, and $E_{\rm therm}$. For each of the multiplicity selections indicated in Fig. 2, the charge and mass of the emitting systems were obtained from Hauger *et al.* [19,20]. Starting with these properties of an average nuclear source we then follow an iterative procedure for comparison of calculated fragment yields and energies to those observed.

Of primary importance is the mean thermal excitation energy $E_{\rm therm}$ of the emitters when fragments freeze-out. The value of $E_{\rm therm}$ was constrained as shown in Fig. 3, by varying the thermal excitation energy of the composite system in the Berlin multifragmentation model to achieve a good match between the absolute experimental and simulated fragment-charge distributions. For multiplicity bin $M3$, Ref. [20] suggests that the average nuclear system ($A\approx 122\pm 10$, $Z\approx 51\pm 4$) has a total initial excitation of $E_i\approx 12\pm 2A$ MeV. It is very important to distinguish the total initial energy E_i of this emission ensemble from its thermal component $E_{\rm therm}$, which is relevant for statistical multifragmentation [18]. From Fig. 3 one finds that (for $A=130$) a value of only 6.2A MeV is required to fit the Z distribution, i.e., $E_{\rm therm}\sim\frac{1}{2}E_i$. This large difference is ascribed to the collective energy associated with expansion as discussed below. A similar fit made for emitters of $A=115$ also requires a value of 6.2A MeV for $E_{\rm therm}$. Since these fits depend mainly on $E_{\rm therm}/A$ one might describe this procedure as the use of a Z distribution thermometer.

Using the emitter characteristics above for bin $M3$, we have performed calculations for several expansion velocities $\beta_{\rm exp}$ for each ejectile charge. Calculated results for $\beta_{\rm exp}=0$ are shown in Fig. 2; for each Z, one assigns $\beta_{\rm exp}$ as required to match the data in Fig. 2. Figure 4(a) shows extracted $\beta_{\rm exp}$ values as a function of charge for multiplicity selections $M3$ and $M1$. These $\beta_{\rm exp}$ values can be said to represent the average best fit collective velocity boosts required to account for the experimental values of $\langle K_t\rangle$ shown in Figs. 2(a) and 2(c) respectively. The results are not significantly changed by using emitter mass of 115 or 130 as described above.

Figure 4(a) shows $\beta_{\rm exp}$ values for bin $M3$ which are substantially larger than those for $M1$. We attribute this difference to the large increase in excitation energy of the average emitters. Apparently, an increase in excitation energy leads to greater internal pressure which leads to larger expansion velocities. The fact that multiplicity bin $M3$ is associated with relatively large $\beta_{\rm exp}$ values as well as the largest IMF multiplicities, suggests that an expanded volume plays an important role in the mechanism for IMF production.

The $\beta_{\rm exp}$ values shown in Fig. 4(a) can be associated with a mean radial collective energy $\langle K_{\rm col}\rangle=\sqrt{(\gamma m\beta_{\rm exp})^2+m^2}-m$ as shown Fig. 4(b) [26]. A decreasing trend of $\beta_{\rm exp}$ with Z is clear for both multiplicity selections, and supports the notion that the general characteristics of collective expansion are similar for both low and high excitation energies. The trends for $\beta_{\rm exp}$ and $\langle K_{\rm col}\rangle$ do not reflect a uniform expansion due, for example, to dynamically driven compression. Such uniform expansion would result in the heaviest fragments carrying the largest collective energy. In addition, the BUU calculations show a total compression energy that does not exceed $\sim$70 MeV. This strengthens the intuitive notion that this collective expansion is mainly driven by nucleonic collisions or ''thermal expansion.''

These values of $\langle K_{\rm col}\rangle$ in Fig. 4(b) represent additional contributions to $\langle K_t\rangle$ which are over and above the normal Coulomb and thermal contributions associated with statistical decay [26]. For multiplicity bin $M1$, these values for $\langle K_{\rm col}\rangle$ are relatively small and independent of Z. For even

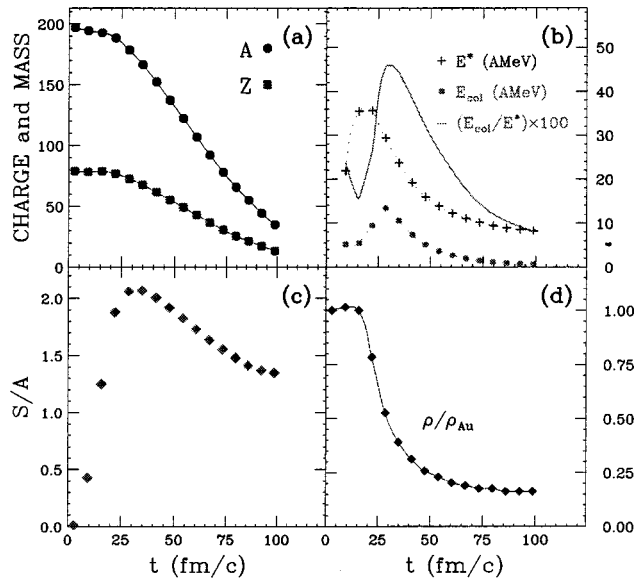

FIG. 5. Time evolution of various emitter properties calculated from BUU [16] for central ($b=0$) collisions.

lower multiplicities values of $\langle K_{\rm col}\rangle$ are smaller still (but have poor statistics). In contrast, the $\langle K_{\rm col}\rangle$ values for $M3$ are large and show a sharp increase with decreasing charge, indicating that here the lighter fragments and particles carry away an increasingly large part of the total expansion energy.

This expansion energy can be evaluated by multiplying the observed values of $\langle K_{\rm col}\rangle$ [Fig. 4(b)] by the average multiplicity of the respective ejectiles for a given multiplicity bin (e.g., Fig. 3). For $M3$ such a procedure yields a collective expansion energy that is $\approx 50\%$ of the total initial energy E_i in the emitting system. This result is consistent with and partially independent of the analysis of the Z distributions in Fig. 3. This large expansion energy clearly demonstrates the important role of thermally driven expansion in the decay mechanism for central Au+C collisions. It is also significant that light particles ($Z=\leqslant 3$) account for the largest fraction of the expansion energy and exit with the largest velocities. The heavier IMF's carry smaller expansion velocities which suggest that they follow behind the lighter ejectiles in time and/or space.

In order to gain a more cinematic view into the dynamic evolution of the Au+C reaction, we have also performed BUU calculations [16] that are similar in spirit to time honored Monte Carlo calculations for the nucleon-nucleon collision cascade [27]. However, BUU includes a self consistent nuclear mean field which follows the evolving nuclear density and is not frozen in shape or size. From these BUU calculations we extract the time dependence of the mass (A), charge (Z), density (ρ), entropy (S), excitation energy (E^*), and total collective energy ($E_{\rm col}$) of the core reaction medium [28]. The position, velocity, mass and size of the core are determined in a self-consistent manner starting from the original Au nucleus. The time evolution of several of the calculated properties is shown in Fig. 5 for central collisions ($b=0$) of $1A$ GeV Au+C.

From Fig. 5 we see a rapid buildup of excitation energy and entropy from nucleonic collisions in the first ~ 25 fm/c. During this time, the collective energy as well as the entropy of the system rise to their respective maxima [see Figs. 5(b) and 5(c)] while the density, Z and A undergo relatively modest changes [see Figs. 5(d) and 5(a) respectively]. Then between ~ 25 and 50 fm/c there is a rapid density decrease and attendant expansion of the reaction system along with a considerable loss of charge, mass, and collective energy, largely via nucleon emission. From ~ 50 to 75 fm/c the mass continues to decrease along with the thermal and collective energies. Intensive properties, density, entropy per nucleon and thermal energy per nucleon decrease rather slowly in this time interval. This latter behavior can be taken as an indication of the final approach toward an essentially thermalized system with average density $\sim 1/4$ to 1/6 of the initial average matter density. It is reasonable that statistical equilibrium could then set in and that freeze-out of the various IMF's could occur in this latter period.

Since the BUU model cannot describe such fragmentation, one must shift to a statistical description for the fragment freeze-out. Can one make this shift in a natural way? The question is not directly answered by the BUU calculations as to when an essentially thermalized system can be said to have been produced. However one may use Fig. 5(a) along with experimental data on total ejectile masses to set bounds on the time assigned for freeze-out. The reconstructed average mass (for $M3$) is $A\approx 122\pm 8\%$ [20] which corresponds to a lower bound of $t\sim 50$ fm/c. The total average IMF mass is $A\approx 80$ which corresponds to an upper bound on the freeze-out time of ~ 80 fm/c. From Fig. 5 one sees an average density of $\frac{1}{4}-\frac{1}{6}$ of the initial density, which is compatible with that used in the multifragmentation statistical model. Total system energy from Fig. 5(b) is compatible with experimental data for $M3$, but the BUU predicts a somewhat smaller fraction of collective energy (for $t>50$ fm/c) compared to our analysis of Figs. 3 and 4.

The data points for $\beta_{\rm exp}$ and $\langle K_{\rm col}\rangle$ in Fig. 4 indicate a fractionation of the collective energy with Z that is reminiscent of the time dependence in Fig. 5(b). However, the dynamical calculations shown in Fig. 5 suggest that the total duration of such collective energy is only up to ~ 80 fm/c. Therefore in this scenario, at times of $\approx 50-80$ fm/c one can conceive of a system possessing radial collective energy but in a steady state near to thermal equilibration; hence, statistical models could be applicable for the fragment freeze-out. The average mass and volume of the reaction core in this time window (50–80 fm/c in Fig. 5) are compatible with the Berlin multifragmentation model as used here (Figs. 2 and 4).

In summary, we have measured the mean transverse kinetic energies of fragments emitted in $1A$ GeV Au+C reactions for a broad range of emitter excitation energies. A large radial expansion is found which cannot be accounted for by the traditional decomposition of the transverse energy into a thermal component and a Coulomb and collective component proportional to the fragment mass. BUU model calculations predict that such extensive collective expansion occurs for $t\sim 25-50$ fm/c after impact; the data indicate a fractionation of this flow energy with Z, the bulk of which is carried away by ejectiles of $Z\leqslant 3$. Subsequent to expansion and cooling, the heavier IMF's emerge with less radial flow from a still hot, low-density nuclear system. Although equipartition of the energy does not occur, a partial equilibration

may well have been achieved prior to multifragment production, which could be reflected in the equilibrium-model descriptions of fragment Z distributions (e.g., Ref. [4]). In this spirit the observed Z distribution is taken as a good thermometer for the low-density nuclear state for freeze-out or multifragmentation.

This work was supported in part by the U.S. Department of Energy under Contracts or Grants No. DE-FG02-87ER40331.A008, DE-AC-03-76SF00098, DE-FG02-89ER40531, DE-FG02-88ER40408, DEFG02-88ER40412, DE-FG05-88ER40437, and by the National Science Foundation under Grant No. PHY-91-23301.

[1] H. Stocker and W. Greiner, Phys. Rep. **137**, 277 (1986).
[2] Q. Pan and P. Danielewicz, Phys. Rev. Lett. **70**, 2062 (1993).
[3] G. Peilert *et al.*, Phys. Rev. C **39**, 1402 (1989).
[4] M. Gilkes *et al.*, Phys. Rev. Lett. **73**, 1590 (1994).
[5] J. Pochodzalla *et al.*, Phys. Rev. Lett. **75**, 1040 (1995).
[6] D. H. E. Gross *et al.*, Nucl. Phys. **A488**, 217c (1988).
[7] W. A. Friedman, Phys. Rev. C **42**, 667 (1990).
[8] *Proceedings of the 1st Catania Relativistic Ion Studies*, edited by S. Costa, S. Albergo, A. Insolia, and C. Tuvè (World Scientific, Singapore, 1996).
[9] S. J. Yennello *et al.*, Phys. Rev. Lett. **67**, 671 (1991).
[10] D. R. Bowman *et al.*, Phys. Rev. Lett. **67**, 1527 (1991).
[11] K. Hagel *et al.*, Phys. Rev. Lett. **68**, 2141 (1992).
[12] W. C. Hsi *et al.*, Phys. Rev. Lett. **73**, 3367 (1994).
[13] S. C. Jeong *et al.*, Phys. Rev. Lett. **72**, 3468 (1993).
[14] D. Heuer *et al.*, Phys. Rev. C **50**, 1943 (1994).
[15] M. Lisa *et al.*, Phys. Rev. Lett. **75**, 2662 (1995).
[16] P. Danielewicz, Phys. Rev. C **51**, 716 (1995).
[17] D. H. E. Gross, Rep. Prog. Phys. **53**, 605 (1990); D. H. E. Gross and K. Sneppen, Nucl. Phys. **A567**, 317 (1994).
[18] J. Lauret, Doctoral Thesis, Université Joseph Fourier, Grenoble, France (1997).
[19] J. A. Hauger *et al.*, Phys. Rev. C, in press.
[20] J. A. Hauger *et al.*, Phys. Rev. Lett. **77**, 235 (1996).
[21] G. Rai *et al.*, IEEE Trans. Nucl. Sci. **37**, 56 (1990).
[22] G. Bauer *et al.*, Nucl. Instrum. Methods Phys. Res. A **386**, 249 (1997).
[23] S. Albergo *et al.*, Nucl. Instrum. Methods Phys. Res. A **311**, 280 (1992); C. Tuvè *et al.*, Phys. Rev. C, in press.
[24] C. A. Ogilvie *et al.*, Phys. Rev. Lett. **67**, 1214 (1991).
[25] The experimental $\langle K_t \rangle$ values shown in panels (a)–(c) are not corrected for detector acceptance as in Ref. [19]. However, the calculated $\langle K_t \rangle$ values do include corrections for the acceptance of the EOS setup. These corrections are negligible for $M3$ and $\approx 12\%$ for $M1$.
[26] Note that it is the transverse component of $\langle K_{\mathrm{col}} \rangle$ which contributes directly to $\langle K_t \rangle$.
[27] Y. Yariv and Z. Fraenkel, Phys. Rev. C **20**, 2227 (1979); **24**, 488 (1991).
[28] The boundary of the reaction medium is defined somewhat intuitively [16]. Quantities shown in Fig. 5 depend only slightly on this definition and stated conclusions are mindful of this mild fuzziness.